Research note

Surface reflectance of sea ice and under-ice irradiance in Kongsfjorden, Svalbard

Jan-Gunnar Winther, Kåre Edvardsen, Sebastian Gerland & Børge Hamre

Initial results from a field experiment on fast ice in Kongsfjorden, Svalbard, in March 2002 are presented. We measured surface reflectance and under-ice irradiance using an advanced, portable spectroradiometer sensitive in the visible and near-infrared parts of the electromagnetic spectrum, i.e. 350 - 1100 nm. Under-ice irradiance (UV-A, UV-B and photosynthetically active radiation [PAR]) was measured down to depths of 7.5 m by vertical profiling using a six-channel radiometer. We also present model results of wavelength-dependent transmittance of radiation through a combined snow and sea ice layer for various thicknesses of snow. Model results show that the snow and sea ice is more transparent for solar radiation in the PAR region (400 - 700 nm) than at shorter and longer wavelengths. This is confirmed by the field measurements. Even very thin snow layers on top of the sea ice efficiently prevent solar radiation from penetrating the snow–sea ice system. For example, a 5 cm thick snow layer reduces under-ice irradiance in the PAR region with a factor of about 10. Measurements of under-ice UV irradiance show that both UV-A and UV-B irradiance is reduced with a factor of more than 10 at depths of 7.5 m below the ice compared to at the ice–sea water interface.

J.-G. Winther & S. Gerland, Norwegian Polar Institute, Polar Environmental Centre, NO-9296 Tromsø, Norway, winther@npolar.no; K. Edvardsen, Norwegian Institute for Air Research, Polar Environmental Centre, NO-9296 Tromsø, Norway; B. Hamre, Dept. of Physics, University of Bergen, Allégaten 55, NO-5007 Bergen, Norway.

Optical properties of snow and sea ice have interested researchers for several decades (e.g. Langleben 1968; Grenfell et al. 1994; Perovich 1994; Winther 1994; Mobley et al. 1998). The crucial role that Svalbard's seasonally ice-covered fjords play in biological productivity dynamics has also been discussed (e.g. Mehlum 1991; Hop et al. 2002). For example, sea ice algae survival depends on radiation penetrating the sea ice and the physical and chemical properties of the water below the sea ice and within brine drainage channels (Horner 1985; Gerland et al. 1999; McMinn et al. 1999). Here we present data on surface reflectance and under-ice irradiation acquired in March 2002 in Kongsfjorden at the west coast of Spitsbergen, Svalbard, at about 79° N (Winther et al. 2002). Some results from a coupled atmosphere –snow–ice–ocean model are also shown (Hamre et al. in press).

Methods

The optical field measurements were performed using a spectroradiometer (FieldSpec, Analytical Spectral Devices Inc., Boulder, CO) that meas-

ures irradiance in the 350 to 2500 nm wavelength region (Quakenbush 1994). The instrument consists of three built-in separate spectrometers. The signal-to-noise ratio decreases considerably in the infrared region. Thus in this research note we present only measurements from the first spectrometer, covering 350 - 1100 nm. When performing the reflectance measurements an 18° field-of-view adapter was used on the sensor, which was mounted on a tripod. The surface reflectance is defined as the ratio between reflected and incident radiation. This relationship was determined by means of calibration measurements using a halon-target reference plate placed at the surface. More precisely, the incident radiation was obtained using this reference plate with known reflectance signature combined with reflected radiation measured of the natural snow (or sea ice) surface (Winther et al. 1999).

For under-ice measurements a waterproof extension fibre was connected to an optical cosine receptor, mounted on a swing arm, which could be operated through a hole drilled through the sea ice cover. After lowering the sensor into the drilled hole the arm was swung out 90° such that the sensor was positioned a few centimetres below the sea ice and about 1 m horizontally away from the drill hole. Consecutive measurements above and below the sea ice with not more than approximately 10 seconds difference and selection of measurements during stable sky conditions lead us to neglect influence of radiation variations due to changing cloud conditions. Additionally, we used a six-channel radiometer (NILU-UV Irradiance Meter, Norwegian Institute for Air Research, Kjeller) with 5 UV channels and one photosynthetically active radiation (PAR) channel (400 - 750 nm) for under-ice measurements down to depths of about 7.5 m. The UV centre wavelengths are 305, 312, 320, 340 and 380 nm, each with a bandwidth of about 10 nm. The NILU-UV radiometer is absolute-calibrated for performance of under-water measurements. Surface irradiance measurements were made in parallel with the under-ice measurements. This allowed us at any time to compensate for changes in light conditions during profiling.

Model experiments were performed using the CASIO-DISORT model that treats shortwave radiation in the Coupled Atmosphere Snow–Ice–Ocean (CASIO) system based on the DIScrete-Ordinate Radiative-Transfer (DISORT) method. Jin & Stamnes (1994) gave a detailed description of the radiative transfer in the CASIO system, including the treatment of the interface conditions. Model simulations using 1998 field data from Kongsfjorden (Gerland et al. 1999) for validation are reported in Hamre et al. (in press).

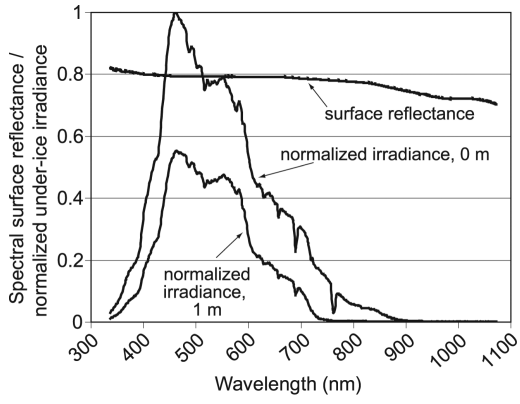

Fig. 1. The curves show average surface sea ice reflectance, normalized under-ice irradiance taken directly below the sea ice and normalized under-ice irradiance taken 1 m below the underside of the ice on 15 March in the inner part of Kongsfjorden. Surface reflectance measurements at wavelengths shorter than about 400 nm are probably artificial and caused by a modest contamination of the reference plate.

Results

Figure 1 shows the average surface reflectance of sea ice covered by a 1 - 2 cm snow layer, normalized under-ice irradiance directly below the sea ice and normalized under-ice irradiance at 1 m below the ice's underside on 15 March 2002, taken in the inner part of Kongsfjorden. First, the relative high surface reflectance (i.e. around 0.8 in the visible part of the electromagnetic spectrum region and with lower values in the near-infrared region) is caused by the snow cover that overlies the less reflective sea ice (Grenfell & Maykut 1977; Grenfell & Perovich 1984; Allison et al. 1993). We think that surface reflectance measurements at wavelengths shorter than about 400 nm are artificial, caused by a modest contamination of the reference plate. Second, the under-ice irradiance measurements at depths of zero and 1 m relative to the underside of the sea ice, respectively, demonstrate that intensities of solar radiation in the PAR region (400 - 700 nm) dominate over those at shorter and longer wavelengths. The PAR at 1 m depth is about 50 % of the intensities directly at

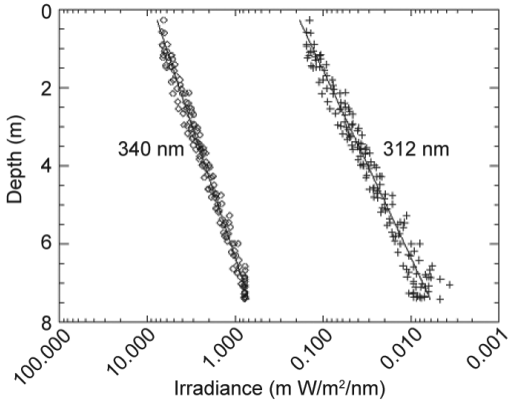

Fig. 2. The curve to the left (340 nm) and the curve to the right (312 nm) are curve fits of the actual data (crosses) assuming the light absorption to follow the equation: $Irr(z) = Irr(0) \cdot \exp(-k \cdot z)$, where z is water depth and k is the attenuation coefficient. Measurements were taken on 15 March under snow-free, 28 cm thick sea ice, with the sun only 15 degrees over the horizon behind a mountain.

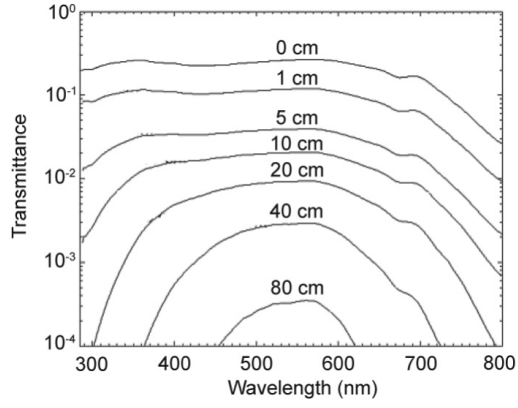

Fig. 3. The curves show modelled transmittance of a combined snow and sea ice layer versus wavelength for snow depths ranging 0 to 80 cm. The sea ice thickness is 60 cm.

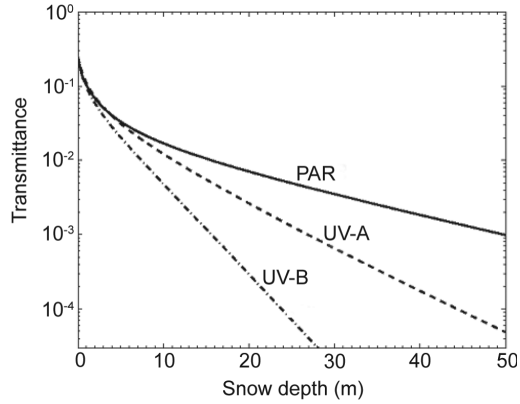

Fig. 4. The figure shows modelled transmittance of a combined snow and sea ice layer for PAR, UV-A and UV-B radiation versus snow depth (0 - 50 cm). The sea ice thickness is 60 cm.

the sea ice–sea water interface (Fig. 1).

Figure 2 illustrates the vertical distribution of UV irradiance over the upper 7.5 m of the seawater (i.e. under-ice irradiance). Both UV-A and UV-B irradiance decrease with a factor of more than 10 (UV-B decreases relatively more than UV-A) at depths of 7.5 m from the underside of the ice compared to at the sea ice–sea water interface. The water contains high concentrations of suspended material originating from the nearby Kongsvegen glacier. Further, the absolute values of irradiance at 340 nm (UV-A) are close to 100 times higher than the absolute values of irradiance at 312 nm (UV-B).

In Fig. 3 we show model calculations of how a snow cover on top of 60 cm sea ice affects the transmittance of radiation through the combined snow and sea ice layer. Two things stand out: first, even a very thin snow layer blocks out most of the solar radiation. For example, a 5 cm thick snow layer reduces the transmittance with a factor of approximately 10. Second, Fig. 3 clearly shows that more of the PAR radiation is transmitted through the snow–sea ice system than at shorter and longer wavelengths, especially for snow depths exceeding 10 cm.

The latter effect is further exemplified in Fig. 4, where transmittance of radiation through 60 cm thick sea ice covered with various thickness of snow is separated for PAR, UV-A and UV-B radiation. As for attenuation in water (see Fig. 2), UV-B irradiance drops more rapidly than UV-A with increasing snow depth. For 60 cm thick sea ice covered with 15 cm of snow, roughly $10^{-3.0}$ (i.e. 1/1000), $10^{-2.4}$ (i.e. 1/250) and $10^{-2.0}$ (i.e. 1/100) of the radiation is transmitted through the snow–sea ice system in the UV-B (280 - 320 nm), UV-A (320 - 400 nm) and PAR wavelength region, respectively.

The results in Figs. 3 and 4 are based on model simulations with input from measurements made in March 2002. Measured snow grain radiuses varied from 0.05 - 0.10 mm in the upper part of the snow to 0.50 - 2.50 mm close to the snow–ice interface. The bulk snow density was measured to 260 kg/m^3. Vertical profiles of sea ice temperature and salinity have also been used. Measured

variables, such as those mentioned above, have been used as input for model simulations, when available. For variables not available, such as particle content that strongly influence on the optical characteristics of sea ice, realistic assumptions based on experience and others' work have been used. We assume that the maximum intensity found between 500 - 600 nm, reflects the presence of algae in the lower part of the sea ice as reported by Gerland et al. (1999). Overall, model results correspond well with in situ measurements as reported by Hamre et al. (in press).

Concluding remarks

We have presented in situ measurements and model results that quantify the solar radiation penetrating the snow–sea ice system depending on wavelength, amount of snow on top of the sea ice and water depth. Most simulations made by General Circulation Models indicate enhancement of both temperature and precipitation in the Arctic. In contrast, Curtis et al. (1998) and Warren et al. (1999) observe a decreasing trend in precipitation for the western and central Arctic. We conclude that too little attention has been drawn to the combined effect of increase in temperature and winter precipitation and its influence on sea ice thickness variability in the Arctic. Our study shows that even small changes in winter precipitation, or amounts of snow, can significantly alter the surface energy balance and the under-ice radiation available for biological production. This work will continue in 2003–06 in the framework of Norwegian–USA collaborative polar research funded jointly by the Research Council of Norway and the US National Science Foundation.

Acknowledgements.—S. Gerland was affiliated with the Norwegian Radiation Protection Authority when this fieldwork was carried out. We acknowledge the Research Council of Norway and our home institutions for their financial support. We thank the personnel at the Norwegian Polar Institute's research station in Ny-Ålesund for their professional and kind assistance during our field campaign.

References

Allison, I., Brandt, R. E. & Warren, S. G. 1993: East Antarctic sea-ice: albedo, thickness distribution, and snow cover. *J. Geophys. Res. 98(C7)*, 12 417–12 429.

Curtis, J., Wendler, G., Stone, R. & Dutton, E. 1998: Precipitation decrease in the western Arctic, with special emphasis on Barrow and Barter Island, Alaska. *Int. J. Climatol. 18*, 1687–1707.

Gerland, S., Winther, J.-G., Ørbæk, J. B. & Ivanov, B. V. 1999: Physical properties, spectral reflectance and thickness development of first year fast ice in Kongsfjorden, Svalbard. *Polar Res. 18*, 275–282.

Grenfell, T. C. & Maykut, G. A. 1977: The optical properties of ice and snow in the Arctic Basin. *J. Glaciol. 18*, 445–463.

Grenfell, T. C. & Perovich, D. K. 1984: Spectral albedos of sea ice and incident solar irradiance in the southern Beaufort Sea. *J. Geophys. Res. 89(NC3)*, 3573–3580.

Grenfell, T. C., Warren, S. G. & Mullen, P. C. 1994: Reflection of solar-radiation by the Antarctic snow surface at ultraviolet, visible, and near-infrared wavelengths. *J. Geophys. Res. 99(D9)*, 18 669–18 684.

Hamre, B., Winther, J.-G., Gerland, S., Stamnes, J. J. & Stamnes, K. in press: Modeled and measured optical transmittance of snow covered first-year sea ice in Kongsfjorden, Svalbard. *J. Geophys. Res. Ocean*.

Hop, H., Pearson, T., Hegseth, E. N., Kovacs, K. M., Wiencke, C., Kwasniewski, S., Eiane, K., Mehlum, F., Gulliksen, B., Wlodarska-Kowalczuk, M., Lydersen, C., Weslawski, J. M., Cochrane, S., Gabrielsen, G. W., Leakey, R. J. G., Lønne, O. J., Zajaczkowski, M., Falk-Petersen, S., Kendall, M., Wängberg, S.-Å., Bischof, K., Voronkov, A. Y., Kovaltchouk, N. A., Wiktor, J., Poltermann, M., di Prisco, G., Papucci, C. & Gerland, S. 2002: The marine ecosystem of Kongsfjorden, Svalbard. *Polar Res. 21*, 167–208.

Horner, R. A. (ed.) 1985: *Sea ice biota*. Boca Raton, FL: CRC Press.

Jin, Z. & Stamnes, K. 1994: Radiative transfer in nonuniformly refracting layered media: atmosphere–ocean system. *Appl. Opt. 33*, 421–442.

Langleben, M. P. 1968: Albedo measurements of an Arctic ice cover from high towers. *J. Glaciol. 7*, 289–297.

McMinn, A., Ashworth, C. & Ryan, K. 1999: Growth and productivity of Antarctic sea ice algae under PAR and UV irradiances. *Bot. Mar. 42*, 401–407.

Mehlum, F. 1991: Breeding population size of the common eider *Somateria mollissima* in Kongsfjorden, Svalbard, 1981–1987. *Nor. Polarinst. Skr. 195*, 21–29.

Mobley, C. D., Cota, G. F., Grenfell, T. C., Maffione, R. A., Pegau, W. S. & Perovich, D. K. 1998: Modeling light propagation in sea ice. *IEEE Trans. Geosci. Remote Sens. 36*, 1743–1749.

Perovich, D. K. 1994: Light reflection from sea ice during the onset of melt. *J. Geophys. Res. 99(C2)*, 3351–3359.

Quakenbush, T. K. 1994: *Extinction of ultraviolet-A, visible and near infrared wavelength light in snow and Antarctic sea ice.* PhD thesis, University of Alaska, Fairbanks.

Warren, S. G., Rigor, I. G., Untersteiner, N., Radionov, V. F., Bryazgin, N. N., Aleksandrov, Y. I. & Colony, R. 1999: Snow depth on Arctic sea ice. *J. Climate 12*, 1814–1829.

Winther, J.-G. 1994: Spectral bi-directional reflectance of snow and glacier ice measured in Dronning Maud Land, Antarctica. *Ann. Glaciol. 20*, 1–5.

Winther, J.-G., Gerland, S., Ørbæk, J. B., Ivanov, B. V., Blanco, A. & Boike, J. 1999. Spectral reflectance of melting snow in a High Arctic watershed on Svalbard: some implications for optical satellite remote sensing studies. *Hydrol. Proc. 13*, 2033–2049.

Winther, J.-G., Godtliebsen, F., Gerland, S. & Isachsen, P. E. 2002: Surface albedo in Ny-Ålesund, Svalbard: variability and trends during 1981–97. *Glob. Planet. Change 32*, 127–139.